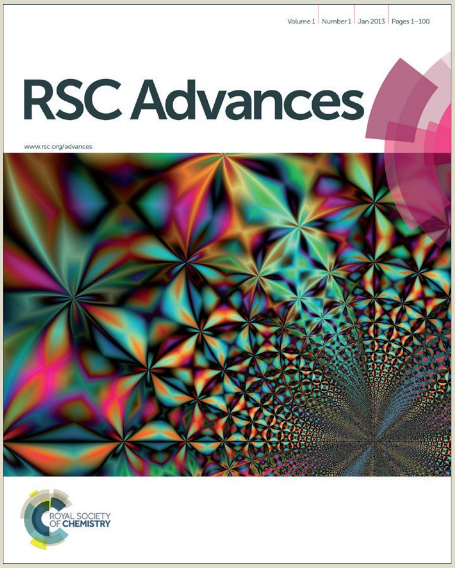
Volume 1 | Number 1 | Jan 2013 | Pages 1–100
RSC Advances
www.rsc.org/advances
ROYAL SOCIETY OF CHEMISTRY

Graphical Abstract

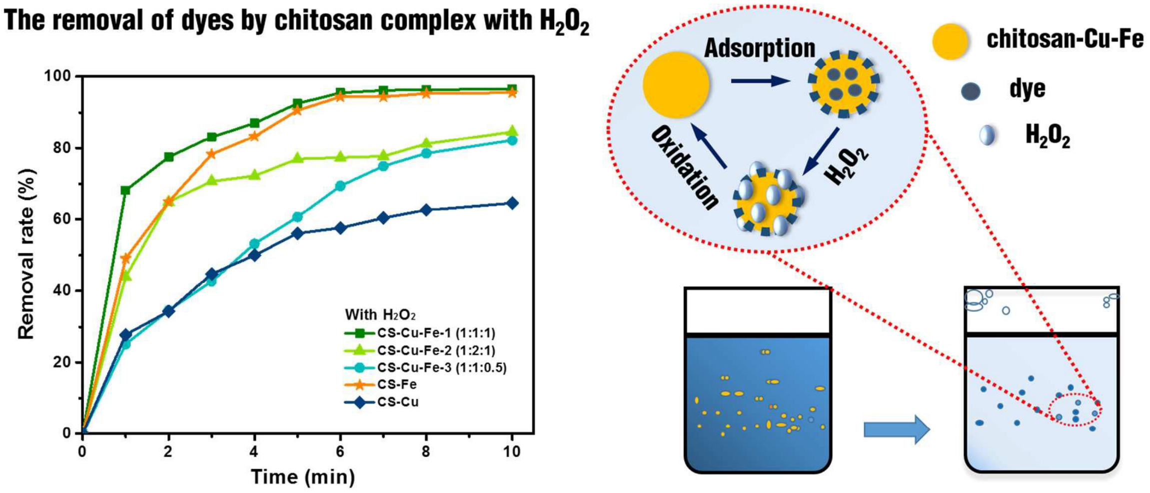

Enhanced catalytic ability of chitosan-Cu-Fe bimetal complex for the removal of dyes in aqueous solution

Sadia Rashid [a, b], Chensi Shen [a, b, *], Xiaoguang Chen [a, b], Su Li [a, b],

Yanhong Chen [a, b], Yuezhong Wen [c], Jianshe Liu [a, b, *]

[a] *College of Environmental Science and Engineering, Donghua University, Shanghai 201620, China.*

[b] *State Environmental Protection Engineering Center for Pollution Treatment and Control in Textile Industry, 201620, China.*

[c] *Institute of Environmental Science, Zhejiang University, Hangzhou 310058, China.*

---

* Corresponding author: Tel: +86-21-6779-2548; Fax: +86-21-67792523.

E-mail address: shencs@dhu.edu.cn (C. S. Shen); liujianshe@dhu.edu.cn (J. S. Liu)

Abstract

In this study, despite the high adsorption ability, efficient catalytic activity of chitosan-metal complex has been developed through the chelation of chitosan polymer with bimetals Cu(II) and Fe(III). The removal of C. I. Reactive Black 5 (RB 5) by chitosan-Cu-Fe complex/H_2O_2 system was studied in the pH range from 4 to 12. The maximal dye removal rate was achieved at an optimal concentration of Cu and Fe in the chitosan-Cu-Fe matrix, demonstrating the combination of sorptive enrichment and catalytic degradation. The results indicated that TOC removal and discoloration of dye achieved 89.9% and 96.5% in a short reaction time. pH sensitivity of chitosan complex, the effect of the coexisting ions and the adsorption of other anionic dyes were also studied. X-ray photoelectron spectroscopy (XPS), Fourier transform infrared spectroscopy (FTIR), scanning electron microscopy (SEM) and energy-dispersive X-ray spectroscopy (EDX) were analyzed to study the structure of chitosan bi-metal complex and the possible mechanism was proposed.

Keywords: Chitosan complex; Dyes removal; Adsorption; Catalytic oxidation; H_2O_2

1. Introduction

According to the literature, 700,000 tons of synthetic dyes and dying materials are produced annually[1], and a large portion of them (about 2~50%) are released into the ecosystem as generated industrial wastewater due to various applications[2, 3]. It is known that wastewaters containing dyes are very difficult to treat since the dyes are recalcitrant molecules, which are resistant to aerobic digestion, and stable to oxidizing agents[4]. To face these current challenges, many non-conventional low-cost adsorbents, including natural materials, biosorbents and waste materials from industries and agriculture have been proposed for the development of cheaper and effective adsorbents[5].

Among these low-cost adsorbents, chitosan, a polysaccharide composed of polymers of glucosamine and N-acetyl glucosamine, has received a great deal of attention due to its advantages, such as biodegradable, nontoxic and high chemical stability[6]. Most importantly, the chemically reactive hydroxyl and amine groups in chitosan make it a versatile candidate for adsorption of dyes[7]. Recently, metal-binding chitosan has received a great deal of attention due to its high efficiency in the removal of contaminants from water. For example, Fe-crosslinked chitosan complex was prepared and used as an efficient adsorbent for the removal of heavy metals from aqueous solutions[8]. Besides, As(V) sorption in the chitosan complexed with different metal ions like Cu(II), Fe(III), La(III), Mo(VI) and Zr(IV) were studied by Shinde and co-workers[9]. Meanwhile, we found that chitosan-Fe(III) could efficiently remove the dyes via chelation between sulfonic groups of the dye and Fe(III) centers in chitosan-Fe(III) complex with high maximum adsorption capacity of 294.5 mg/g under pH 12[4].

Although chitosan-metal complexes have shown high performance for pollutant adsorption, some limitations still exist. During the regeneration of adsorbents, large amount of strong acid or alkaline elution reagents need to be used, which may induce secondary pollution and even produce large amounts of solid wastes due to the leftovers of used adsorbents. Unlike adsorption, advanced oxidation processes (AOPs) are promising technologies for the treatment of wastewaters containing non-easily removable organic compounds, because they can effectively mineralize the contaminants or transform them into harmless products[10, 11]. Correspondingly, chitosan-Cu(II) complex was found to catalyze H_2O_2 for the degradation of azo dyes and the •OH radical played the main role in dye oxidation. But this rate of dye oxidation depends directly on the dye structure and the removal efficiency of the dye with large molecular weight still needs to be improved[12]. Chitosan-TiO_2 has been used to enhance the photocatalytic activity of chitosan composite for the degradation of the dyes[13, 14]. Besides, silver, gold and platimum nanoparticles were also synthesized in chitosan for improved catalyst formation[15, 16]. If this kind of catalytic activity of chitosan metal composite can be combined with high adsorption ability, the naturally abundant biopolymer will imply attractive potential on dye removal processes.

Recently, many researchers concluded that the adsorption ability of catalyst support also contribute a lot to the catalytic efficiency enhancement[17]. For example, Guo et al. reported that the enhancement of the degradation activity of TiO_2/Na-HZSM-5 was attributed to the adsorption of the dye by the medium strong acid sites in the zeolitic supports[18]. Gonzalez-Olmos et al. indicated that the stronger adsorptive enrichment of MTBE on the Fe-Beta zeolite played a positive role for the degradation reaction[19]. Meanwhile, Han et al. reported that Cu^{2+} and Fe^{3+} ions have synergetic effect in the bimetal modified PAN fibers for dye degradation[20]. Considering the cost of the materials, we planned to prepare a kind of bimetal chitosan complex in order to combine the catalytic activity of chitosan-Cu(II) with the high adsorption ability of chitosan-Fe(III).

Herein, a kind of chitosan-Cu-Fe bimetal complex was proposed for the removal of dyes with H_2O_2. The removal efficiency of dye pollutants was evaluated in view of kinetics and isotherms of RB 5 adsorption, the heterogeneous catalytic oxidation by chitosan complex, pH sensitivity of chitosan complex, effect of the coexisting ions, adsorption of other anionic dyes and reusability experiments. The possible mechanism proposed in this study may also be used to account for the high efficiency of dye removal by chitosan bimetal complex.

2. Materials and Methods

2.1. Chemicals

Glutaraldehyde, $CuSO_4 \cdot 5H_2O$, $FeCl_3 \cdot 6H_2O$ and ethanol were attained from National Medicines Corporation Ltd. of China. Chitosan was purchased from Zhejiang Golden-shell Biochemical Co., Ltd, Zhejiang, China (deacetylation degree = 91.04%). Reactive Black 5 (RB 5) and other dyes were bought from Sigma-Aldrich. During all experiments, doubly distilled water was used and other chemicals were of laboratory reagent grade which were used without any further purification.

2.2 Preparation of Chitosan Metal Complex

Chitosan-Cu-Fe complex was prepared by the following procedure[21]. Chitosan powder (0.83 g) was dissolved in 50 mL water containing 0.4 mL acetic acid. Subsequently, 0.1 mol/L $FeCl_3 \cdot 6H_2O$ aqueous solution, and 0.1 mol/L $CuSO_4 \cdot 5H_2O$ aqueous solution (50 mL) were added into dissolved chitosan and the mixture was stirred at room temperature for 4 h. Next, the chitosan-Cu-Fe complex precipitation was obtained after the addition of ethanol (150 mL). The solid was then washed with ethanol to remove the excess of $FeCl_3$ and $CuSO_4$, and finally dried at 80°C. Chitosan-Cu-Fe complex powders were prepared with different ratios of copper and iron as given in Table 1. It is well known that the high hydrophilicity of chitosan due to the primary amine group makes chitosan easily soluble in dilute acid solutions to yield a hydrogel in water[22]. The swelling characteristics of chitosan hydrogels are dominated by the nature of the polymer and the state of water[23, 24]. In our study, when the Fe^{3+} ions bonded to chitosan polymer with a relative high ratio (the molar ratio of chitosan, Cu(II), Fe(III) in chitosan-Cu-Fe complexes are 1:1:2 and 1:0.5:1), chitosan complex became swelling, which might be due to the changes of the chitosan structures. The less swelling behavior of chitosan complex was important so they can be used in column research for our further studies. Therefore, we chose the less swelling bimetal complexes and studied their catalytic properties. For simplicity, here after these catalysts are abbreviated as CS-Cu-Fe-1, CS-Cu-Fe-2 and CS-Cu-Fe-3. Additionally, chitosan-Cu and chitosan-Fe complexes were prepared by modifying this procedure (Text S1 in supporting information). Here after chitosan-Cu and chitosan-Fe will be mentioned as CS-Cu and CS-Fe for simplicity's sake.

2.3. Removal Procedures of dyes

Dye removal experiments were performed using 100 mL flasks, which were sealed and agitated at 100 rpm in a thermostatic shaker maintained at 25 °C. The typical reaction mixture was initiated with 50 mL of dye at 100 mg/L and 0.1 g of the chitosan complex. The catalytic oxidation of RB 5 and other different dyes were carried out in a 100 mL flasks in the presence of H_2O_2. During pH study, the initial pH value of the dye solution were adjusted from 4 to 12 by addition of 0.01 mol/L HCl and 0.01 mol/L NaOH, respectively. The reusability experiment of chitosan complex was performed with the same conditions, and the dyes were added after each catalytic degradation experiment.

2.4. Characterization

Fourier Transform Infrared Spectroscopy (FTIR) of chitosan complexes were recorded by a Shimadzu 8900-FTIR spectrometer (Shimadzu, Japan) using KBr power containing ca. 1% (w/w) of sample. *X-ray Photoelectron Spectroscopy (XPS) Analysis* of the CS-Cu, CS-Fe and CS-Cu-Fe complex was performed on a Thermo ESCALAB 250 electron spectrometer (Thermo Electron, US). The samples were excited with X-rays over a specific 400 μm area using monochromatic Al Kα radiation (1486.6 eV) at 150 W. Due to the maximum measurable depth of XPS is less than 20 nm, it could not detect the background signal in our analysis. The XPS spectra were fitted assuming Gaussian-Lorentzian distribution for each peak, with a linear background in order to determine the binding energy of the various element core levels, and all binding energies were referenced to the neutral carbon peak at 284.8 eV. All of the XPS spectra were normalized. The surface morphology of chitosan-Cu-Fe complex was examined using the scanning electron microscopy (SEM) Quanta 250 (FEI, USA)) equipped with an energy-dispersive X-ray spectrometer (EDX) X-Max 80 (Aztec, Oxford).

2.5. Analysis

Dye concentrations were analyzed using a Shimadzu UV-2401PC UV-vis spectrometer (Shimadzu, Japan) at its absorbance maximum. H_2O_2 content was measured by photometric measurements using the solution of titanyl sulfate[25] and Shimadzu UV-2401PC UV-vis spectrometer (Tokyo, Japan) at its absorbance maximum. TOC (total organic carbon) analysis was performed using a Shimadzu TOC-V CPH (Shimadzu, Japan), aliquots of 10 mL sample were periodically withdrawn, filtrated through 0.22 μm syringe filter and measured immediately.

3. Results and Discussion

3.1. Effect of Cu and Fe ions in the polymer matrix of chitosan

CS-Cu, CS-Fe and CS-Cu-Fe (1, 2 and 3) were prepared with different ratios of Fe and Cu in the polymer matrix (Table 1). It can be observed from the Figure 1a that RB 5 adsorption on CS-Cu-Fe-1 was a very fast process (88.6%) as compared with two other complexes CS-Cu-Fe-2 (57.6%) and CS-Cu-Fe-3 (53.6%), and reached equilibrium in 10 min. Whereas in the presence of H_2O_2 (Figure 1b), the concentration of RB 5 in CS-Cu-Fe-1 and CS-Cu-Fe-2 group declined very rapidly in the first 5 min, finally contributing to 96.5% and 84.6% removal efficiency, and approached the equilibrium in about 10 min. While in the case of CS-Cu-Fe-3, where it was a very slow process but eventually reached equilibrium with the removal efficiency as 82.2 %. In the group of initial chitosan, the adsorption efficiency of RB 5 reached 32.2% in 10 min, while the concentration of RB 5 declined 38.5% in the presence of H_2O_2, which was little higher than the adsorption efficiency. Meanwhile, clear difference can be seen in adsorption (17.1%) and oxidation (64.6%) properties of CS-Cu complex, where as CS-Fe have very little difference between adsorption (93%) and oxidation (95.5%), indicating the high adsorption capacity of CS-Fe complex and the evident catalytic activity of CS-Cu.

From these results, noteworthy conclusions were derived. The catalytic activity and the adsorption ability of the CS-Cu-Fe-1 complex depends directly on the content of Cu and Fe ions. It’s clear from the graph that adsorption efficiency of CS-Fe complex (93.1%) is greater than CS-Cu complex (17.1%) which supports the fact that complex CS-Cu-Fe-1 (88.6%) have greater adsorption efficiency due to the presence of Fe in the complex as compared to Cu. While, CS-Cu-Fe-2 (1:2:1) and CS-Cu-Fe-3 (1:1:0.5) which have higher ratio of Cu content as compared to Fe content showed the adsorption efficiencies as 57.6% and 53.6% respectively. Thus, the presence of more copper and less iron content have contributed to lower the adsorption efficiency of these two complexes. On the other hand, during oxidation reaction in the presence of H_2O_2, higher removal efficiencies of 96.5% (CS-Cu-Fe-1), 84.6% (CS-Cu-Fe-2) and 82.2% (CS-Cu-Fe-3) confirm that the catalytic properties of these three complexes are due to the presence of copper. Thus, Cu content is responsible for increased dye removal rate by the CS-Cu-Fe (1, 2 and 3) complexes in the presence of H_2O_2. But when Cu content is more as compared to Fe, it decreases the amount of adsorbed dye. Therefore, the maximal dye removal rate can be achieved at an optimal concentration (CS-Cu-Fe-1 (1:1:1)) of Cu and Fe in the chitosan-Cu-Fe matrix, which shows the combination of sorptive enrichment and catalytic degradation.

3.2. Kinetics and Isotherms of RB 5 adsorption by chitosan complex

Rapid interaction of the pollutants to be removed is desirable and beneficial for practical adsorption applications. The kinetic adsorption behavior of the dye removal process without H_2O_2 was studied at different initial dye concentrations using CS-Cu-Fe-1 (Figure 2a). It is observed from the figure that the adsorption of RB 5 by CS-Cu-Fe-1 was a very fast process and approached the adsorption equilibrium in about 10 min. Besides, the total amount of RB 5 adsorbed increased with the increasing initial dye concentrations. In order to further determine mass transfer mechanism and factors which are responsible for rate controlling, kinetic data were correlated to linear forms of the pseudo-first-order rate model and the second-order rate model (Text S2 in supporting information). By correlating kinetic data with two rate models, it was observed that high degree of nonlinearity suggests the incapability of the pseudo-first-order model to describe the kinetic profile of the adsorption process, whereas it was found that the plot of t/q_t against time using different initial dye concentrations for adsorption process gives straight lines (Figure 2b) with high correlation coefficients (Table S1 in supporting information). This shows that the present sorption system follows chiefly the second-order rate model and gives the impression that this reaction is controlled by chemisorption[26].

The adsorption isotherm of RB 5 on chitosan complex under various initial dye concentrations in the presence of 0.05g/L of the CS-Cu-Fe-1 powder was measured. Freundlich, Langmuir and Langmuir-Freundlich isotherms were used to fit the experimental data (Text S3 in supporting information). The results of the experimental data were fitted to these three equations and the results are shown in Figure 3. The Langmuir-Freundlich isotherm fits best with the experimental data (correlation coefficient $R^2 = 0.9743$), whereas the low correlation coefficients ($R^2 = 0.9278$) show less agreement of Freundlich isotherm with the experimental data. The sorption capacity of the CS-Cu-Fe-1 was found to be 527.3305 mg/g according to Langmuir-Freundlich equation and this value is very high so far reported in previous literatures as compared to other sorption capacities of chitosan adsorbents.

3.3. Heterogeneous catalytic oxidation with chitosan complex

The effect of various initial dye concentrations on the degradation of RB 5 in the presence of CS-Cu-Fe-1/ H_2O_2 were also analyzed. Even at various initial dye concentrations (Figure 4a), the removal efficiency was above 80%. The effect of various H_2O_2 concentrations on the degradation of the dye in the presence of CS-Cu-Fe-1 were also analyzed, showing an increase of removal efficiency with the increase of H_2O_2 concentration. Figure 4(b) shows the removal efficiency of RB 5 was 86.3% with a volume of 0.1 mL hydrogen peroxide and achieving a degradation higher than 90% when the volume of hydrogen peroxide was increased up to 0.6 mL. With increasing the concentrations, H_2O_2 itself may become a relevant consumer of hydroxyl radicals. The observed trend cannot be arbitrarily extrapolated rather the existence of an optimum H_2O_2 concentration is to be expected.

Figure 5a shows the decomposition of H_2O_2 at various time intervals with CS-Fe, CS-Cu and CS-Cu-Fe-1. The decomposition of H_2O_2 in the presence of CS-Fe nearly remained constant which confirms that H_2O_2 decomposition is negligible during the dye removal process. Whereas in the presence of CS-Cu and CS-Cu-Fe-1, the concentration of H_2O_2 continuously decreased with the increase of time interval. While in the presence of CS-Cu-Fe-1, the decomposition of H_2O_2 was highest after 6 hours. This decomposition of H_2O_2 in the presence of the catalyst CS-Cu and CS-Cu-Fe-1 may be attributed to the catalytic properties of copper in chitosan complex.

As Figure 5b shows, the decomposition of H_2O_2 on CS-Fe, CS-Cu and CS-Cu-Fe-1 followed pseudo-first-order kinetics. The catalytic activity (A) expressed as

$$A = \frac{k_1}{C_{cat}} \qquad (1)$$

The catalytic activity of CS-Cu-Fe-1 and CS-Cu from the pseudo-first-order rate constant (k_1) of the reaction and the catalyst concentrations (C_{cat}) are 3.29×10^{-3} L/g·min and 1.50×10^{-3} L/g·min for H_2O_2 decomposition. For CS-Fe, it is lower by about one order of magnitude (3.54×10^{-4} L/g·min). The present data helps us to assume that H_2O_2 is decomposed at Cu sites on CS-Cu-Fe-1 and CS-Cu, thus resulting in the formation of hydroxyl radicals[25, 27-30]. And these hydroxyl radicals result in the oxidation of organic dyes which are adsorbed on catalyst or dissolve in water. H_2O_2 decomposition with CS-Cu and CS-Cu-Fe-1 cannot be simply explained by the total amount of Cu content alone or both Cu and Fe present in these catalyst (Table 1). Although Fe sites in CS-Fe complex showed lower catalytic activity, its speciation effect which is reflected in CS-Cu-Fe complexes cannot be ignored.

3.4. pH Sensitivity of chitosan complex

The influence of pH on the adsorption of RB 5 was studied by evaluating the performance of adsorbent at pH values 4, 6, 8, 10 and 12. The removal ratio of RB 5 for different pH was shown in Figure 6a. It was observed that the removal ratio of dye by CS-Cu-Fe-1 increased significantly with the decrease of pH from 8 to 4 and decreased with the increase of pH from 8 to 12. One reason behind this decrease is that free amino groups of chitosan under alkaline conditions were not protonated as a result the electrostatic interactions could not play their part between negatively charged anionic dye and chitosan. Therefore, it can be deduced that chelating interactions play the main role between CS-Cu-Fe complex and dye molecules instead of electrostatic interactions.

Further, it can be observed that the reaction can proceed at a wide pH range from acidic to alkaline in the CS-Cu-Fe-1/H_2O_2 catalytic system (Figure 6b). Even though, lower pH resulted in higher oxidation rate. This outcome is distinctive from the Fenton system where the oxidation can only take place at pH lower than 3. The removal efficiency increased at all pH conditions from 4 to 12 with removal efficiency greater than 80 % and with highest removal efficiency at pH 4 as 94%. It is important to indicate that catalytic degradation of RB 5 in CS-Cu-Fe-1/H_2O_2 system was independent of the pH.

3.5. Structure study of chitosan-metal complex

The SEM of CS-Cu-Fe-1 are shown in Figure 7a and 7b at different magnification. It illustrates that the shape of the complex powders are irregular and relatively nonporous. The EDX analysis data for the CS-Cu-Fe-1 is shown in Figure 7c, which confirms the presence of Cu and Fe in these complexes.

The Fourier-transform infrared (FT-IR) spectra of pure chitosan, CS-Cu, CS-Fe and CS-Cu-Fe-1 are shown in Figure 8, respectively. For pure chitosan, a strong and broad absorbent band centered at 3458 cm^{-1} is ascribed to hydroxyl asymmetrical stretching vibration and –NH$_2$ stretching vibration[31]. The absorption band at 1643 cm^{-1} is assigned as amide I vibrations. The absorption band at 1394 cm^{-1} is caused by the coupling of–C–N–stretching vibration, and the band which appears at 1085 cm^{-1} corresponds to the stretching of –C–O– bond. The absorption band at 588 cm^{-1} is due to –N–H stretching vibration[32, 33]. FTIR spectrum of CS-Cu, CS-Fe and CS-Cu-Fe-1 complex show much similar bands of chitosan. The major differences were: the wide peak at 3458 cm^{-1}, corresponding to the stretching vibration of hydroxyl, amino and amide groups became weaker and sharper which indicated the strong interaction between these groups and copper or iron.

X-ray photoelectron spectroscopy (XPS) is used to identify particular elements and to determine the valence state of metals dispersed. To further investigate the interactions among Fe, Cu and chitosan, XPS studies of chitosan before and after chelation of copper and/or iron were conducted. The high-resolution N 1s XPS spectra of different types of chitosan are shown in Figure 9. There are three N1s peaks located at 399.8 eV, 400.8 eV and 401.8 eV for initial chitosan, which are attributed to the existence of the nitrogen atoms in the –NH$_2$, NH–C=O and –NH$_3^+$ groups, respectively. While, a new sub-bands around 398.8 eV was found in the spectrum of CS-Cu, CS-Fe and CS-Cu-Fe-1 complex which might be attributed from the interaction between –NH$_2$ group and Cu^{2+} or Fe^{3+} metal ions[34-36]. Through detailed peak fitting using the XPS peak software package, the peak intensities were assigned to the existence of C-metal (C-M, 530.9 eV) arranged in the following order: CS-Fe > CS-Cu-Fe-1 > CS-Cu, which indicated that Fe ions were more likely to bond with –NH$_2$ groups of chitosan. The peak intensity of –NH$_3^+$ group could be arranged in the following order: CS-Cu-Fe-1 > CS-Cu > CS-Fe, suggesting that the bimetal chitosan complex have the most protonated amine group (–NH$_3^+$). For the spectrum of O 1s, the band of the initial chitosan was composed of two sub-bands, which are attributed to the existence of OH, or bound H_2O (532.6 eV) and the –O– in the ring and possibly –O– between the rings (531.9 eV) which exist in chitosan structure[4, 37]. While in case of chitosan-metal complexes (CS-Fe, CS-Cu, and CS-Cu-Fe -1), new sub-bands at the lower energy (around 530.9 eV) were found in the spectrum of complex, which might be attributed from the interaction between oxygen atom and metal[38]. Different from the interaction between $–NH_2$ group and metals, the peak intensity of –OH could be arranged in reverse order: CS-Cu > CS-Cu-Fe-1 > CS-Fe, indicating that the Cu ions were more likely to bond with $–NH_2$ groups of chitosan. Meanwhile, the high-resolution XPS spectra of the Fe 2p and Cu 2p region are also shown in Figure 9. Fe $2p_{1/2}$ and Fe $2p_{3/2}$ line peaks are located at 724.6 and 711.5 eV, which are the characteristic peaks of Fe(III) and satellite, respectively[39]. Additionally, Cu $2p_{1/2}$ and Cu $2p_{3/2}$ line peaks are located at 953.3 and 933.6 eV, which are the characteristic peaks of Cu(II) and satellite, further suggesting that both Fe(III) and Cu(II) chelate with the chitosan polymer.

According to the literature Bhatia et al. and Hernandez et al.[40, 41] and our previous work, chitosan-Fe(III) complex is hexacoordinated and there is entrance of two or three moles of monomeric sugar units of the ligand in the coordination sphere of Fe^{3+}. The complexation is mainly through the amino group ($–NH_2$) and the hydroxyl group (–OH) of chitosan. Water molecules or other ions in solution would complete the coordination sphere of chitosan-Fe(III) complex with different stability. According to the literature reported by Rhazi et al., two structures for chitosan-Cu(II) have been proposed as $\{[Cu(–NH_2)]^{2+}, 2OH^-, H_2O\}$ and $\{[Cu(–NH_2)_2]^{2+}, 2OH^-\}$[42]. From 5.0 ~ 5.8 pH range the first complex is more stable and for pH values larger than 5.8 the second structure is more predominant. In our study, the pH of the solution was acidic due to addition of acetic acid and $FeCl_3$ so the formation of second type of chitosan structure is ruled out. Lu et al. proposed that the optimized interaction structure of chitosan-Cu complex was tetracoordinated and copper(II) was coordinated with $–NH_2$, C_3–OH and H_2O[43]. By combining the FTIR and XPS results above, we speculated that Fe(III) was hexacoordinated to chitosan molecules, complexing through equal O and N atoms of the chitosan polymer and water molecule, while Cu(II) was tetracoordinated to chitosan molecules and chelated with more O atoms than N atoms of the chitosan polymer (Figure 10).

3.6. Effect of the Coexisting Ions and Adsorption of Other Anionic Dyes

The fact that practically in industries high concentration of salts are also applied to enhance the bath dye exhaustion, which cannot be neglected in this study[44]. Different salts were added to the dye solution under optimal experimental conditions (salt concentration: 50 mg/L, 100 mg/L and 200 mg/L) and the results were shown in Figure 11. The influences of NaCl, $NaNO_3$, $MgSO_4$, KCl, and $CaCl_2$ on RB 5 removal was negligible, suggesting that these common coexisting salts almost had no negative effect on dye removal by CS-Cu-Fe-1 bimetal complex in the presence of H_2O_2. From a practical point of view, these results imply that CS-Cu-Fe-1 complex can be used for the removal of RB 5 from salt-containing wastewaters. The complicated structures of dye molecules which vary with respect to the organic chains and the numbers and positions of functional groups is directly related to their adsorption behaviors. Thus, the same conditions as RB 5 removal were applied to other two different anionic dyes, C. I. Acid Red 73 and C. I. Reactive Blue 19 which showed the removal efficiency of 97.38% and 92.39%.

3.7. The Reusability of chitosan-Cu-Fe complex

The reusability of the new catalyst cannot be ignored for practical applications and economic demand[45]. Figure 12 shows the reusability of CS-Cu-Fe-1 complex on catalytic degradation of RB 5 in the presence of H_2O_2. Results show that the removal efficiency was above 80 % even after 15 cycles indicating that CS-Cu-Fe-1 complex had good reusability and is suitable for practical applications.

3.8. A Possible Mechanism

According to our previous studies, chitosan-Fe(III) complex efficiently removed the dyes via chelation between sulfonic group of dye and Fe(III) center in chitosan-Fe(III) complex [4]. Meanwhile, the above structural study suggests that the addition of Cu(II) had no significant effect on the interaction between Fe(III) and chitosan polymer. In CS-Cu-Fe-1 bimetal complex, Fe(III) was still hexacoordinated to chitosan molecules, complexing through equal O and N atoms of the chitosan polymer and water molecule while Cu(II) was tetracoordinated to chitosan molecules and chelated with more O atoms than N atoms of the chitosan polymer. Hence, it could be induced that the chelating interactions play an important role in dyes adsorption. The electrostatic interactions between protonated amine groups ($–NH_3^+$) in chitosan with the sulfonate groups ($–SO_3^-$) of RB 5 also account much for dye adsorption.

In order to extend the application of chitosan-Fe(III) complex with catalytic property, chitosan-Cu-Fe bimetal complex was prepared. The reported study shows that the matrix of heterogeneous chitosan is able to stabilize and retain isolated Cu^{2+} ions in highly unsaturated coordinative state[46]. Further, Kucherov et al. reported that chitosan-Cu complex is a kind of heterogeneous catalysts for the decolourisation of azo dyes[12]. Nevertheless, there was still room for further improvement in removal efficiency of chitosan-Cu(II) complex. Different from chitosan-Fe(III) complex, the adsorption ability of chitosan-Cu(II) was quite low (Figure 1a) due to its coordination structure. When the Fe(III) ions have been introduced to the chitosan-Cu(II) complex, its adsorption efficiency increased noticeably (Figure 1a) and the removal efficiency of chitosan-Cu-Fe bimetal complex in the presence of H_2O_2 increased accordingly (Figure 1b). In the group of CS-Cu-Fe-1, the removal efficiency of RB 5 reached nearly 80% in only 2 minutes. According to the study reported by Gonzalez-Olmos et al. sorptive enrichment of the contaminant on the surface of the catalyst might lead to higher rate and a more efficient utilization of the formed hydroxyl radicals in contaminant degradation[19]. Additionally, Guo et al. highlighted the significance of the reversible adsorption of the substrate by support improved photocatalytic activity of supported catalyst. Hence, we speculated that the good adsorption ability of chitosan-Fe(III) could promote the catalytic activity of chitosan-Cu(II). In Figure 1b, CS-Cu-Fe-1 shows the higher removal efficiency in first 2 minutes than both CS-Fe and CS-Cu complex, suggesting that the appropriate combination of Fe(III) and Cu(II) ions in chitosan bimetal complex could achieve high efficiency of dye removal.

Further, we employed active species trapping experiment by using methanol as the scavenger for ·OH radical. Figure 13 shows that the addition of excessive methanol made the degradation efficiency decreased, putting it almost on same rate with efficiency in adsorption test. The scavenging effects of excessive methanol on the RB 5 degradation suggested that the major oxidative species in the system were hydroxyl radicals both in the system of CS-Cu-Fe-1 and CS-Cu. These results are corresponding with the results of the published study where the hydroxyl radicals have played an important role in chitosan-Cu catalytic degradation[12]. Similar results have been reported by Han and coworkers. They prepared a kind of Cu-Fe bimetal AO-PAN complexes, which exhibited high activity and stability for the oxidative decomposition of the dye because of the existence of synergetic effect. And the important origin of synergetic effect in Cu–Fe bimetal AO-PAN complexes is considered as the joint action of copper and iron species facilitating the Fe^{3+}/Fe^{2+} cycle and exciting the Cu^{2+}/Cu^{+} redox, followed by the increase in the •OH radicals generation[20].

The removal of total organic carbon (TOC) of chitosan-metal complex/H_2O_2 system was also measured. The results showed that TOC removal rate of dye under CS-Cu/H_2O_2 and CS-Cu-Fe-1/H_2O_2 systems reached 49.5% and 89.9% respectively, while the TOC of CS-Cu/H_2O_2 and CS-Cu-Fe-1/H_2O_2 systems without dye were only 1.33 and 1.18 mg/L after 30 minutes reaction, which indicated that the chitosan-metal complex polymers were stable under this oxidative condition.

4. Conclusion

Despite the high adsorption ability, efficient catalytic activity of chitosan-metal complex has been developed through the chelation of chitosan polymer with bi-metals Cu(II) and Fe(III). It efficiently remove the dyes (> 90% removal rate in 10 minutes) under wide range of pH (pH=4~12) via combination of catalytic activity and high adsorption ability of chitosan bimetal complex. The effect of Cu and Fe ions in the polymer matrix of chitosan, pH sensitivity of chitosan complex, the effect of the coexisting ions, adsorption of the anionic dyes and the reusability have been studied. Further, the possible mechanism for dye removal was also proposed. This technically feasible, highly efficient and cost effective material is very attractive for dyeing effluent treatment. The challenge for research to figure out the detailed catalytic mechanism needs to be further studied in our future work.

Acknowledgments

The authors acknowledge financial support from the National Natural Science Foundation of China (No. 21407021), the Shanghai Yang-Fan Program of Science and Technology Commission of Shanghai (No. 14YF1405000), the Cultivation Fund of the Key Scientific and

Technical Innovation Project, Ministry of Education of China (NO. 708052), the Fundamental Research Funds for the Central Universities, and DHU Distinguished Young Professor Program.

Literature Cited

1. H. Zhu, R. Jiang, Y. Q. Fu, J. H. Jiang, L. Xiao and G. M. Zeng, *Appl Surf Sci*, 2011, **258**, 1337-1344.
2. R. Christie, *Environmental aspects of textile dyeing*, Elsevier, 2007.
3. G. M. Nabil, N. M. El-Mallah and M. E. Mahmoud, *J Ind Eng Chem*, 2014, **20**, 994-1002.
4. C. S. Shen, Y. Shen, Y. Z. Wen, H. Y. Wang and W. P. Liu, *Water Res*, 2011, **45**, 5200-5210.
5. G. Crini, *Bioresource Technol*, 2006, **97**, 1061-1085.
6. C. S. Shen, Y. Z. Wen, X. D. Kang and W. P. Liu, *Chem Eng J*, 2011, **166**, 474-482.
7. R. S. Blackburn, *Environ Sci Technol*, 2004, **38**, 4905-4909.
8. A. C. Zimmermann, A. Mecabo, T. Fagundes and C. A. Rodrigues, *J Hazard Mater*, 2010, **179**, 192-196.
9. R. N. Shinde, A. K. Pandey, R. Acharya, R. Guin, S. K. Das, N. S. Rajurkar and P. K. Pujari, *Water Res*, 2013, **47**, 3497-3506.
10. R. Andreozzi, V. Caprio, A. Insola and R. Marotta, *Catal Today*, 1999, **53**, 51-59.
11. M. Pera-Titus, V. Garcia-Molina, M. A. Banos, J. Gimenez and S. Esplugas, *Appl Catal B-environ*, 2004, **47**, 219-256.
12. R. Sulakova, R. Hrdina and G. M. B. Soares, *Dyes Pigments*, 2007, **73**, 19-24.
13. M. H. Farzana and S. Meenakshi, *Ind Eng Chem Res*, 2014, **53**, 55-63.

14. A. El Kadib, K. Molvinger, C. Guimon, F. Quignard and D. Brunel, *Chem Mater*, 2008, **20**, 2198-2204.

15. D. W. Wei, Y. Z. Ye, X. P. Jia, C. Yuan and W. P. Qian, *Carbohyd Res*, 2010, **345**, 74-81.

16. M. J. Laudenslager, J. D. Schiffman and C. L. Schauer, *Biomacromolecules*, 2008, **9**, 2682-2685.

17. R. Gonzalez-Olmos, M. J. Martin, A. Georgi, F. D. Kopinke, I. Oller and S. Malato, *Appl Catal B-environ*, 2012, **125**, 51-58.

18. P. Guo, X. S. Wang and H. C. Guo, *Appl Catal B-environ*, 2009, **90**, 677-687.

19. R. Gonzalez-Olmos, U. Roland, H. Toufar, F. D. Kopinke and A. Georgi, *Appl Catal B-environ*, 2009, **89**, 356-364.

20. Z. B. Han, Y. C. Dong and S. M. Dong, *J Hazard Mater*, 2011, **189**, 241-248.

21. R. B. Hernandez, A. P. Franc, O. R. Yola, A. Lopez-Delgado, J. Felcman, M. A. L. Recio and A. L. R. Merce, *J Mol Struct*, 2008, **877**, 89-99.

22. E. Ahad, *J Appl Polym Sci*, 1978, **22**, 1665-1676.

23. M. N. Khalid, F. Agnely, N. Yagoubi, J. L. Grossiord and G. Couarraze, *Eur J Pharm Sci*, 2002, **15**, 425-432.

24. K. D. Yao, W. G. Liu and J. Liu, *J Appl Polym Sci*, 1999, **71**, 449-453.

25. J. Mendham, R. Denney, J. Barnes and M. Thomas, *Singapore Ltd, Patparganji, Indian Delh*, 2002, **357**.

26. S. Chatterjee, S. Chatterjee, B. P. Chatterjee, A. R. Das and A. K. Guha, *J Colloid Interf Sci*, 2005, **288**, 30-35.

27. D. J. Doocey and P. N. Sharratt, *Process Saf Environ Prot*, 2004, **82**, 352-358.

28. K. Fajerweg, J. N. Foussard, A. Perrard and H. Debellefontaine, *Water Sci Technol*, 1997, **35**, 103-110.

29. H. Kušić, N. Koprivanac and I. Selanec, *Chemosphere*, 2006, **65**, 65-73.

30. R. Gonzalez-Olmos, U. Roland, H. Toufar, F. D. Kopinke and A. Georgi, *Appl Catal B-environ*, 2009, **89**, 356-364.

31. W. Sajomsang, P. Gonil and S. Tantayanon, *Int J Biol Macromol*, 2009, **44**, 419-427.

32. Z.-s. Cai, Z.-q. Song, S.-b. Shang and C.-s. Yang, *Polym. Bull.*, 2007, **59**, 655-665.

33. H. Li, Y. Du, X. Wu and H. Zhan, *Colloids Surf-A*, 2004, **242**, 1-8.

34. J. M. Nieto, C. Penichecovas and J. Delbosque, *Carbohyd Polym*, 1992, **18**, 221-224.

35. M. T. Klepka, N. Nedelko, J. M. Greneche, K. Lawniczak-Jablonska, I. N. Demchenko, A. Slawska-Waniewska, C. A. Rodrigues, A. Debrassi and C. Bordini, *Biomacromolecules*, 2008, **9**, 1586-1594.

36. Z. Ai, Y. Cheng, L. Zhang and J. Qiu, *Environ Sci Technol*, 2008, **42**, 6955-6960.

37. E. Z. Kurmaev, S. Shin, M. Watanabe, R. Eguchi, Y. Ishiwata, T. Takeuchi, A. Moewes, D. L. Ederer, Y. Gao, M. Iwami and M. Yanagihara, *J Electron Spectrosc*, 2002, **125**, 133-138.

38. J. Qu, Q. L. Hu, K. Shen, K. Zhang, Y. L. Li, H. Li, Q. R. Zhang, J. Q. Wang and W. Q. Quan, *Carbohyd Res*, 2011, **346**, 822-827.

39. T. Yamashita and P. Hayes, *Appl Surf Sci*, 2008, **254**, 2441-2449.

40. S. C. Bhatia and N. Ravi, *Biomacromolecules*, 2000, **1**, 413-417.

41. R. B. Hernández, A. P. Franco, O. R. Yola, A. López-Delgado, J. Felcman, M. A. L. Recio and A. L. R. Mercê, *J Mol Struct*, 2008, **877**, 89-99.

42. M. Rhazi, J. Desbrieres, A. Tolaimate, M. Rinaudo, P. Vottero, A. Alagui and M. El Meray, *Eur Polym J*, 2002, **38**, 1523-1530.

43. R. Q. Lu, Z. G. Cao and G. P. Shen, *J Mol Struc-theochem*, 2008, **860**, 80-85.

44. S. W. Won, G. Wu, H. Ma, Q. Liu, Y. Yan, L. Cui, C. Liu and Y.-S. Yun, *J Hazard Mater*, 2006, **138**, 370-377.

45. H. M. Sun, L. Y. Cao and L. H. Lu, *Nano Research*, 2011, **4**, 550-562.

46. A. V. Kucherov, N. V. Kramareva, E. D. Finashina, A. E. Koklin and L. M. Kustov, *J Mol Catal A-chem*, 2003, **198**, 377-389.

Table 1. The molar ratio of CS, Cu(II), Fe(III) of prepared chitosan-Cu-Fe complexes

Chitosan complex	Ratio	Stability in water
CS-Cu-Fe-1	1:1:1	Stable
CS-Cu-Fe-2	1:2:1	Stable
CS-Cu-Fe-3	1:1:0.5	Stable
CS-Cu-Fe-4	1:1:2	Swelling
CS-Cu-Fe-5	1:0.5:1	Swelling

Figure Captions

Figure 1. The effect of Cu and Fe ions in the polymer matrix of chitosan on the removal of RB 5 (a) adsorption reaction (initial concentration 100 mg/L, 50 mL, chitosan complex 0.1g, T = 25°C, pH = 6.5); (b) catalytic oxidation (initial concentration 100 mg/L, 50 mL, chitosan complex 0.1g, 0.4 mL H_2O_2, T = 25°C, pH = 6.5).

Figure 2. Adsorption kinetics of dyes (initial concentrations ranged from 50 mg/L to 300mg/L, 50 mL) with CS-Cu-Fe-1 complex (0.05 g); (a) time profile showing adsorption process with pseudo first order; (b) fitting curve of adsorption process with pseudo-second order.

Figure 3. Adsorption isotherms fitted to Langmuir model (the dotted line), Freundlich equation (the dashed line) and Langmuir-Freundlich model (the real line).

Figure 4. (a) The effect of various initial dye concentrations (ranged from 50 to 300 mg/L, 50 mL) on RB 5 oxidation in the presence of CS-Cu-Fe-1 (0.05 g) with H_2O_2 (0.4 mL); (b) The effect of H_2O_2 concentration (ranged from 0.1 to 0.6 mL) on RB 5 oxidation (initial concentration 100 mg/L, 50 mL) in the presence of CS-Cu-Fe-1 (0.05g).

Figure 5. (a) Decomposition of H_2O_2 (C_0 = 80 mmol/L) in chitosan complex suspension (initial concentration of dye is 100 mg/L, 50 mL, chitosan complex 0.05g, pH = 6.5, T = 25°C); (b) fitting curve of the decomposition of H_2O_2 with pseudo-first-order model.

Figure 6. pH sensitivity of (a) CS-Cu-Fe-1 complex without H_2O_2; (b) CS-Cu-Fe-1 complex with H_2O_2 (initial concentration of dye 100 mg/L, 100 mL, T=25°C, chitosan complex 0.05g, H_2O_2 0.4 mL, pH = 6.5).

Figure 7. SEM-EDX of CS-Cu-Fe-1 at different magnifications.

Figure 8. FTIR spectra of pure chitosan, CS-Cu, CS-Fe, CS-Cu-Fe-1 chitosan complex.

Figure 9. N 1s (a), O 1s (b), Fe 2p (c), and Cu 2p (d) XPS spectra of pure chitosan, CS-Cu, CS-Fe, CS-Cu-Fe-1 complex.

Figure 10. Proposed chemical structure of chitosan-Cu-Fe bimetal complex.

Figure 11. Effect of the coexisting ions on the removal efficiency of the dye in the presence of CS-Cu-Fe-1 with H_2O_2 (initial concentration ranged from 50 mg/L to 200 mg/L, T = 25°C, 50 mL, adsorbent 0.05g, 0.4 mL H_2O_2, pH = 6.5).

Figure 12. Effect of adsorbent reusability on the catalytic degradation and removal percentage (chitosan complex dose 0.1 g, T = 25°C, initial concentration 100 mg/L, 50 mL, 0.4 mL H_2O_2, pH = 6.5).

Figure 13. Effect of methanol and role of hydroxyl radical on the oxidative degradation of the dye in the presence of CS-Cu-Fe-1 (a) and CS-Cu (b) (initial dye concentrations 100 mg/L, 50 mL, T = 25°C, chitosan complex 0.1g, 0.4 mL H_2O_2, pH = 6.5).

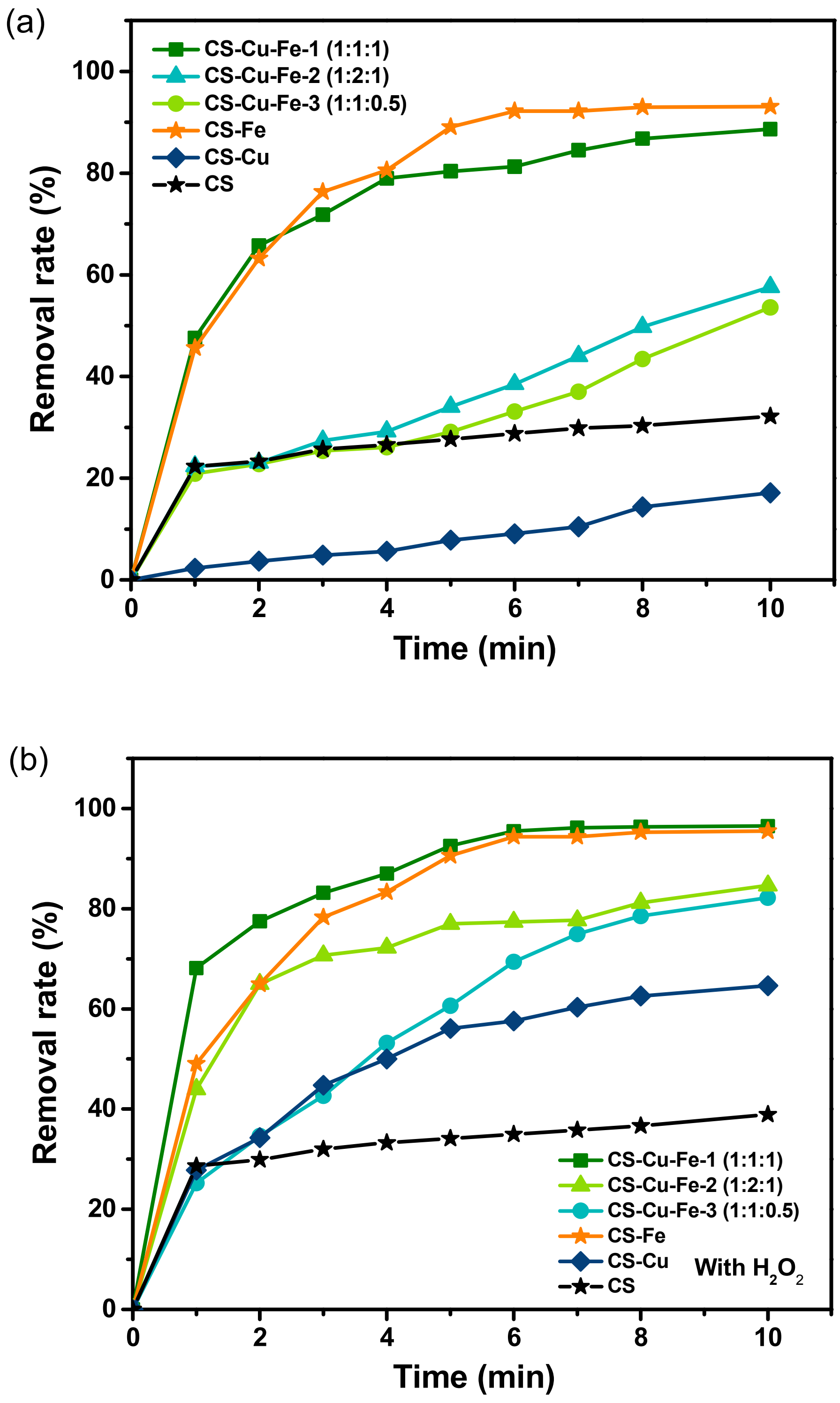
(a)
CS-Cu-Fe-1 (1:1:1)
CS-Cu-Fe-2 (1:2:1)
CS-Cu-Fe-3 (1:1:0.5)
CS-Fe
CS-Cu
CS
Removal rate (%)
0
20
40
60
80
100
Time (min)
0
2
4
6
8
10
(b)
CS-Cu-Fe-1 (1:1:1)
CS-Cu-Fe-2 (1:2:1)
CS-Cu-Fe-3 (1:1:0.5)
CS-Fe
CS-Cu
CS
With H_2O_2
Removal rate (%)
0
20
40
60
80
100
Time (min)
0
2
4
6
8
10

Figure 1

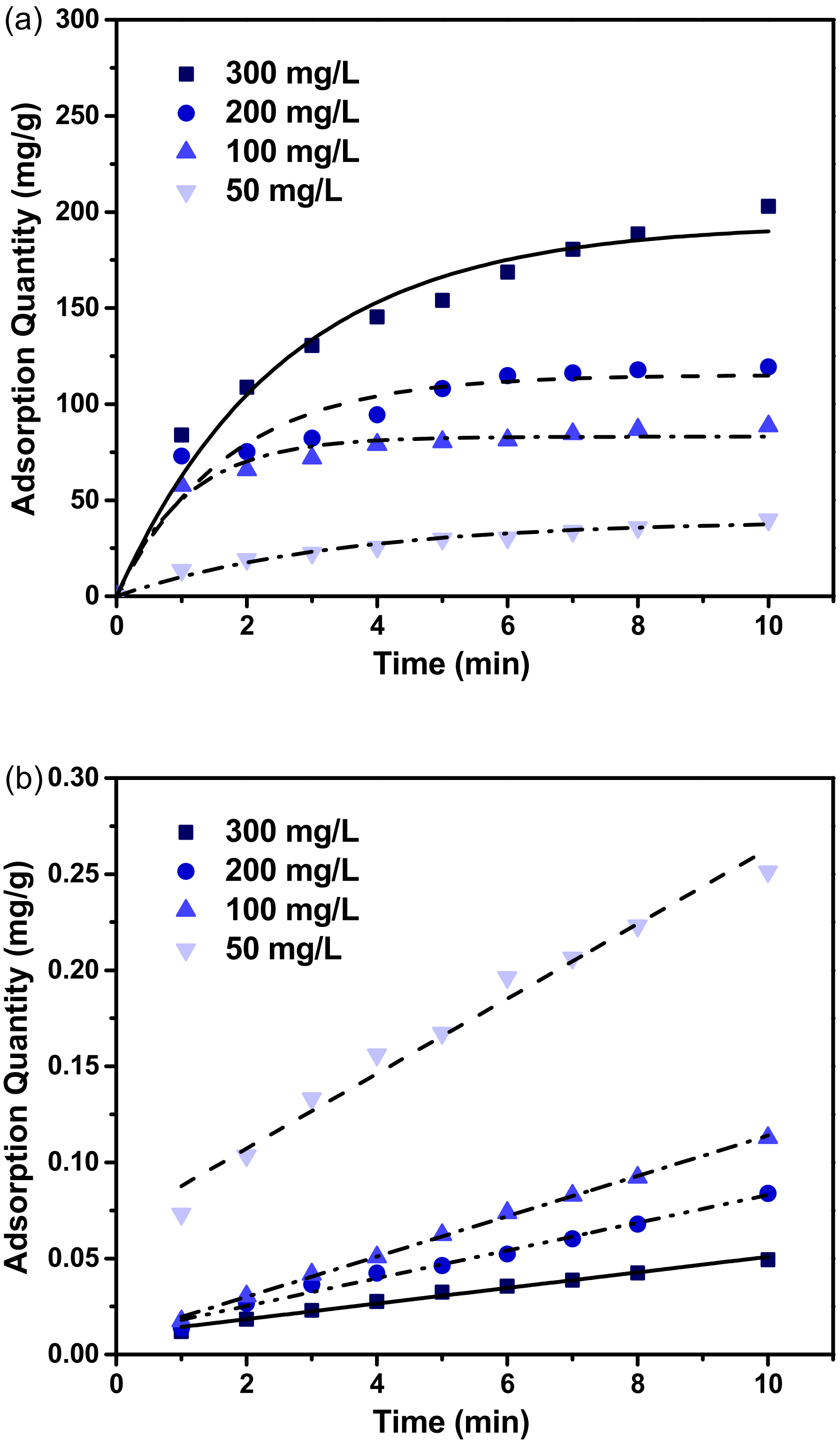
(a)
300 mg/L
200 mg/L
100 mg/L
50 mg/L
Adsorption Quantity (mg/g)
0
50
100
150
200
250
300
Time (min)
0
2
4
6
8
10
(b)
300 mg/L
200 mg/L
100 mg/L
50 mg/L
Adsorption Quantity (mg/g)
0.00
0.05
0.10
0.15
0.20
0.25
0.30
Time (min)
0
2
4
6
8
10

Figure 2

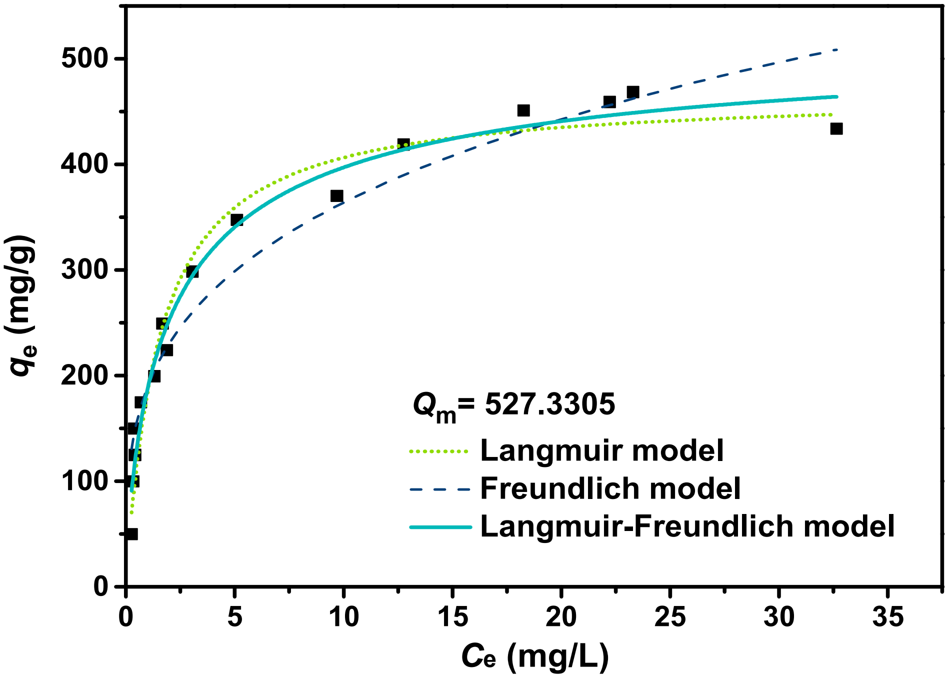
q_e (mg/g)
0
100
200
300
400
500
0
5
10
15
20
25
30
35
C_e (mg/L)
Q_m= 527.3305
Langmuir model
Freundlich model
Langmuir-Freundlich model

Figure 3

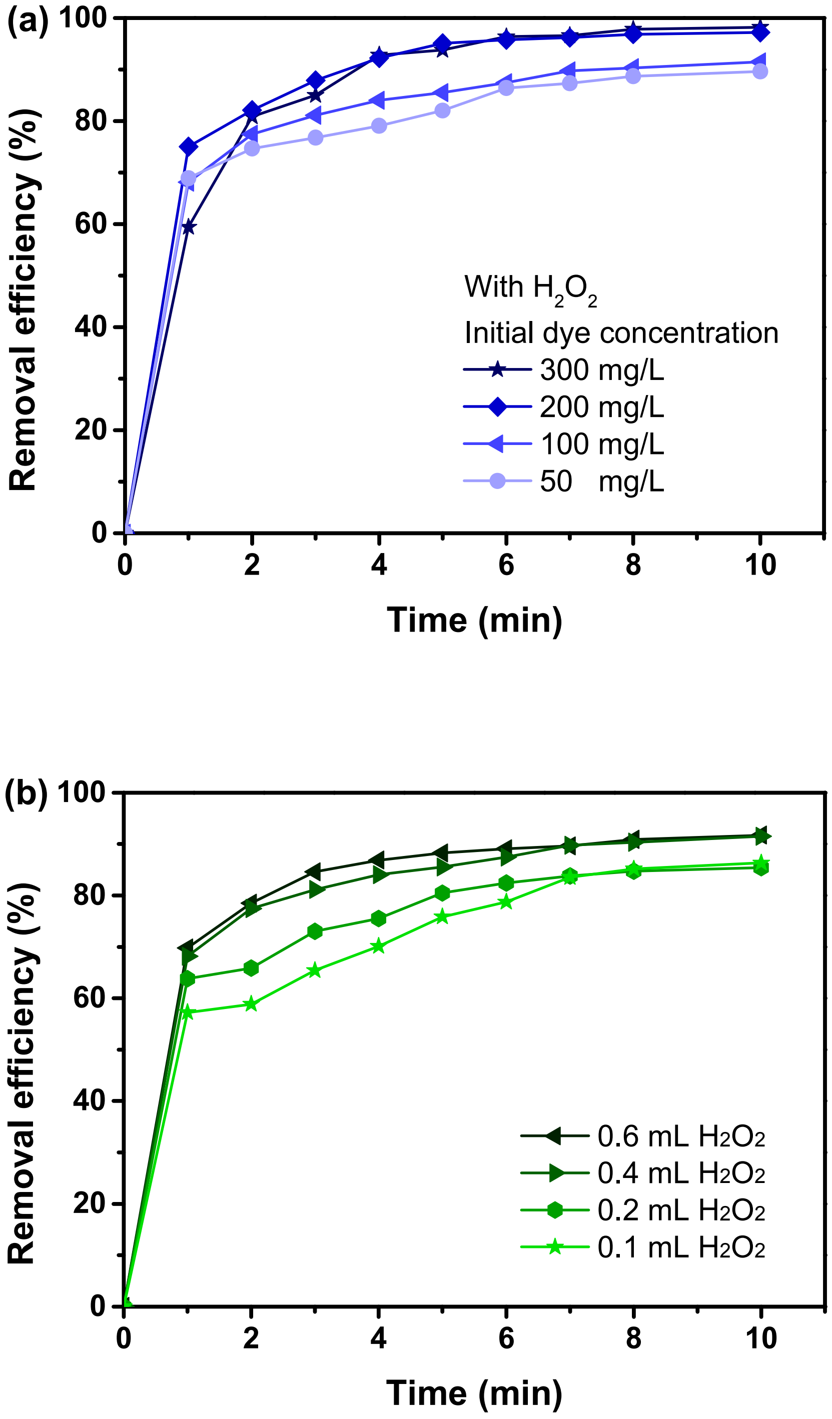
(a)
Removal efficiency (%)
Time (min)
0
20
40
60
80
100
0
2
4
6
8
10
With H_2O_2
Initial dye concentration
300 mg/L
200 mg/L
100 mg/L
50 mg/L
(b)
Removal efficiency (%)
Time (min)
0
20
40
60
80
100
0
2
4
6
8
10
0.6 mL H_2O_2
0.4 mL H_2O_2
0.2 mL H_2O_2
0.1 mL H_2O_2

Figure 4

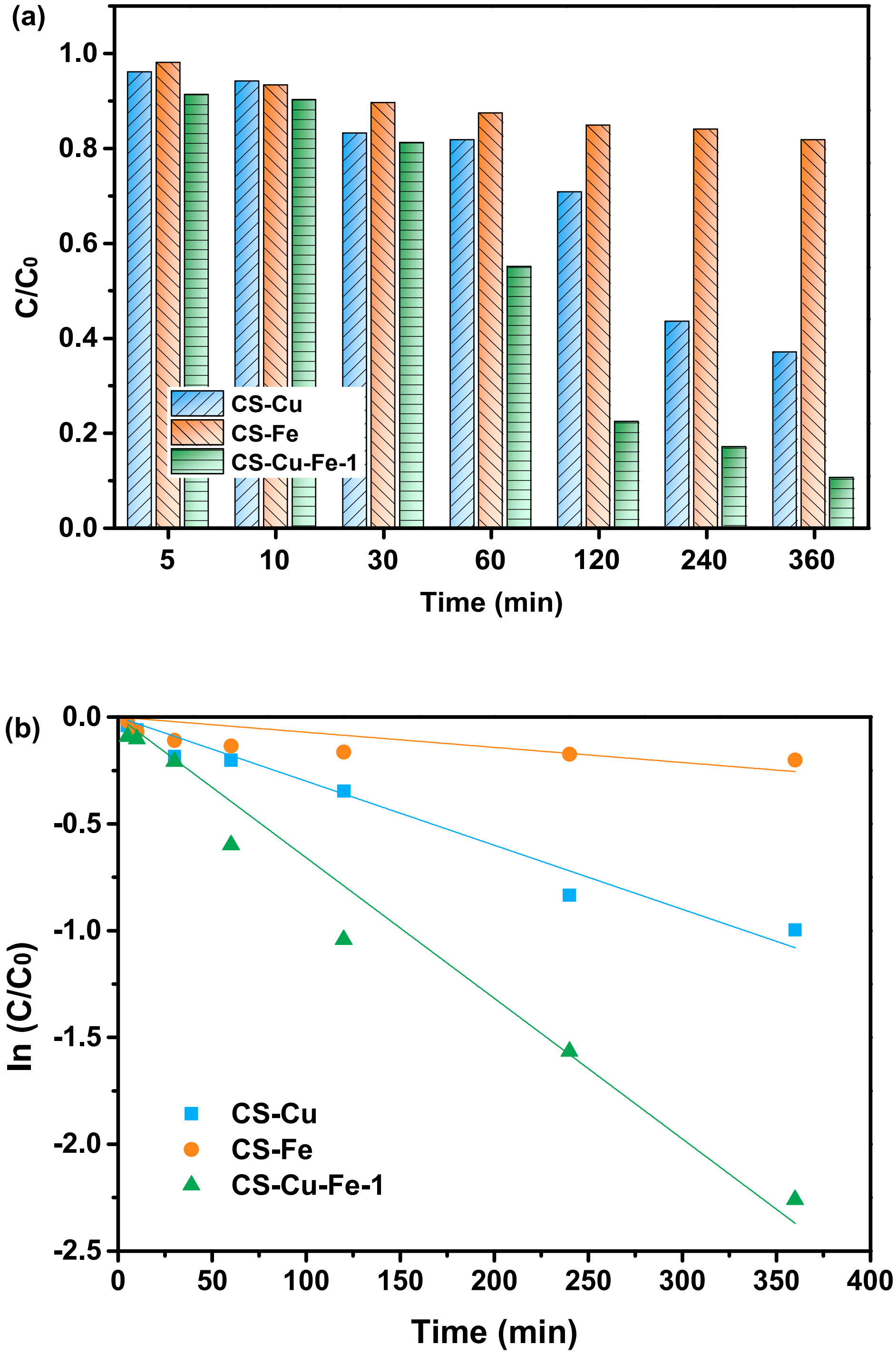
(a)
C/C₀
1.0
0.8
0.6
0.4
0.2
0.0
CS-Cu
CS-Fe
CS-Cu-Fe-1
5
10
30
60
120
240
360
Time (min)
(b)
ln (C/C₀)
0.0
-0.5
-1.0
-1.5
-2.0
-2.5
CS-Cu
CS-Fe
CS-Cu-Fe-1
0
50
100
150
200
250
300
350
400
Time (min)

Figure 5

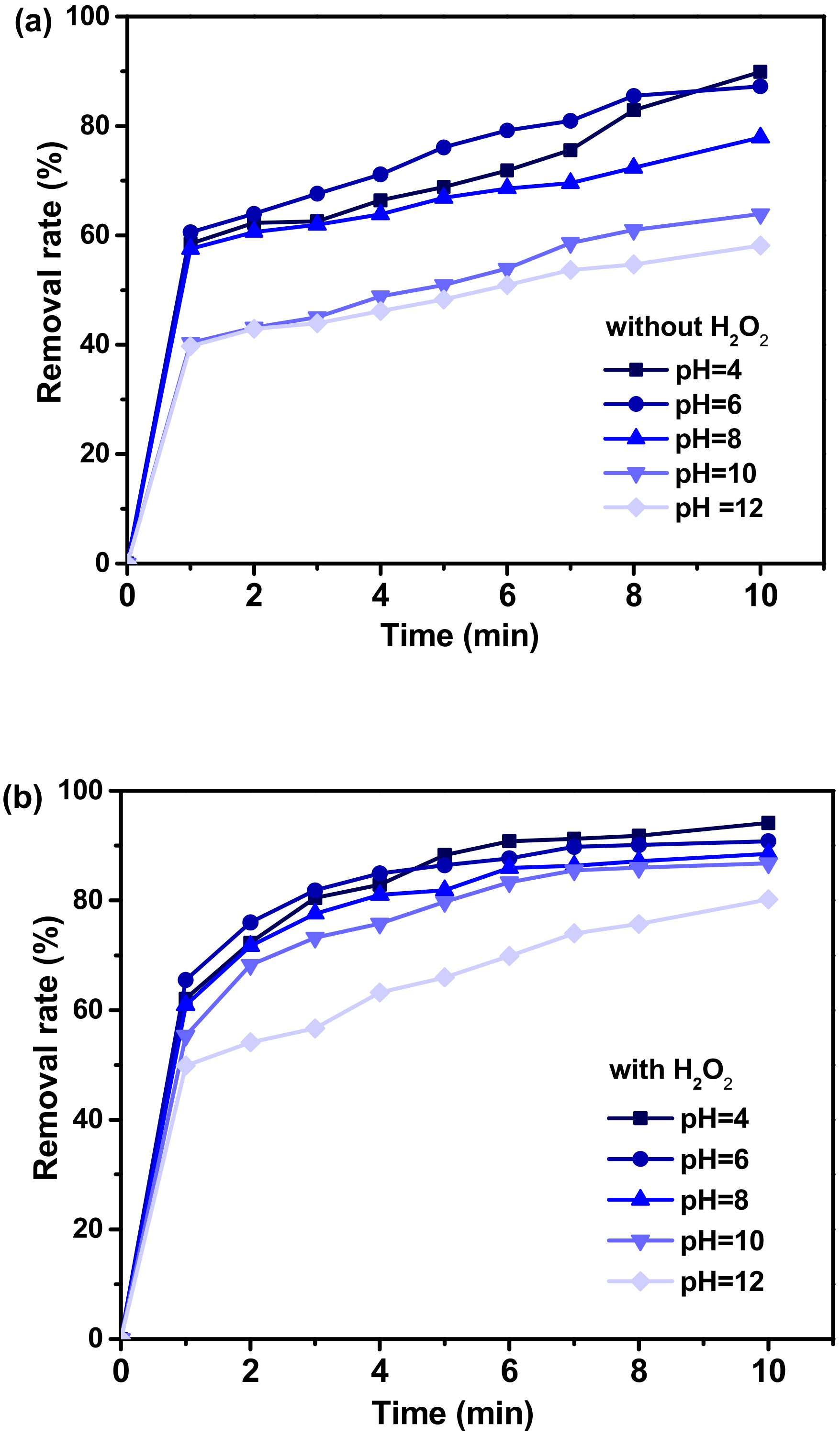
(a)
Removal rate (%)
0
20
40
60
80
100
Time (min)
0
2
4
6
8
10
without H_2O_2
pH=4
pH=6
pH=8
pH=10
pH =12
(b)
Removal rate (%)
0
20
40
60
80
100
Time (min)
0
2
4
6
8
10
with H_2O_2
pH=4
pH=6
pH=8
pH=10
pH=12

Figure 6

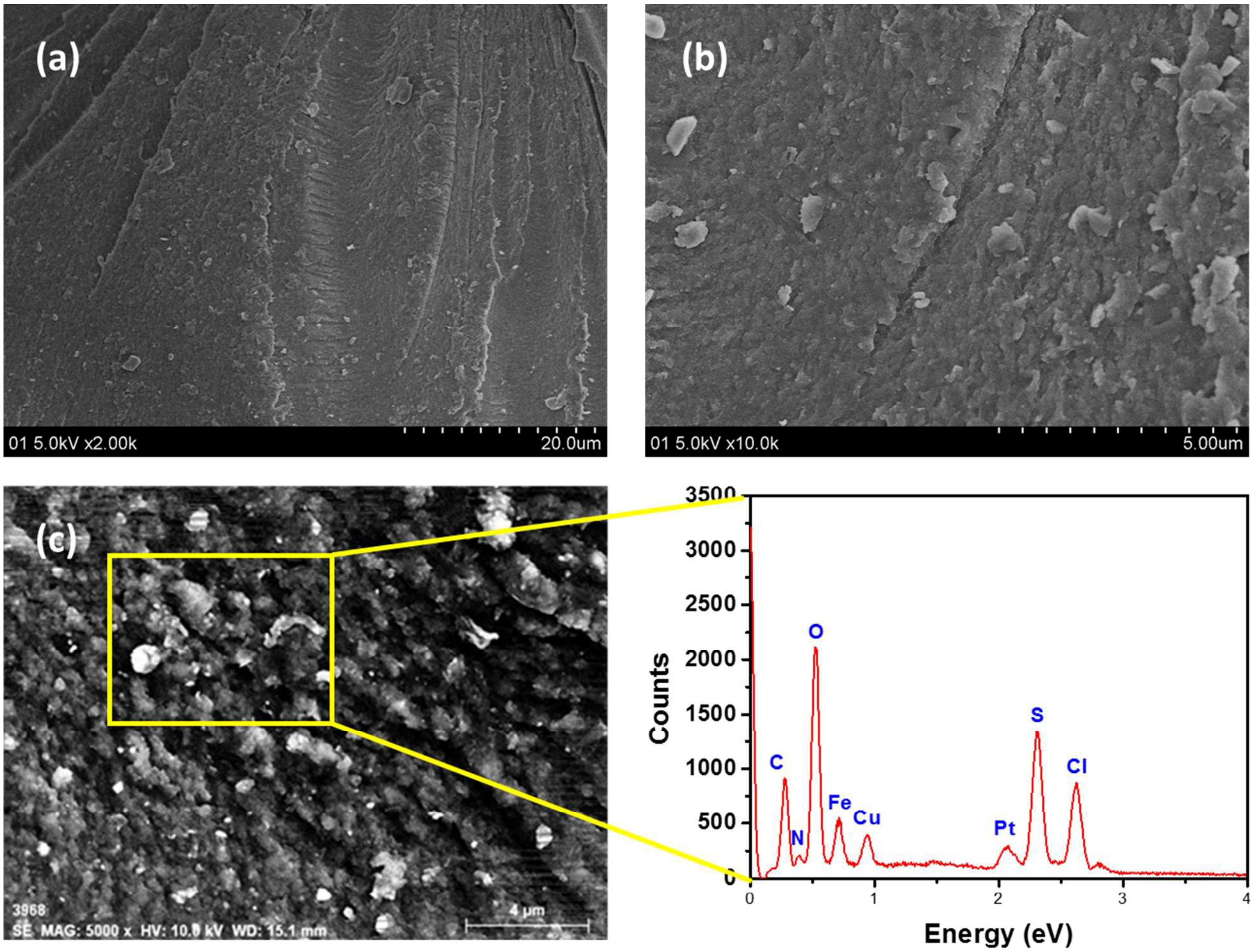
(a)
01 5.0kV x2.00k
20.0um
(b)
01 5.0kV x10.0k
5.00um
(c)
3968
SE MAG: 5000 x HV: 10.0 kV WD: 15.1 mm
4 μm
Counts
0
500
1000
1500
2000
2500
3000
3500
Energy (eV)
0
1
2
3
4
C
N
O
Fe
Cu
Pt
S
Cl

Figure 7

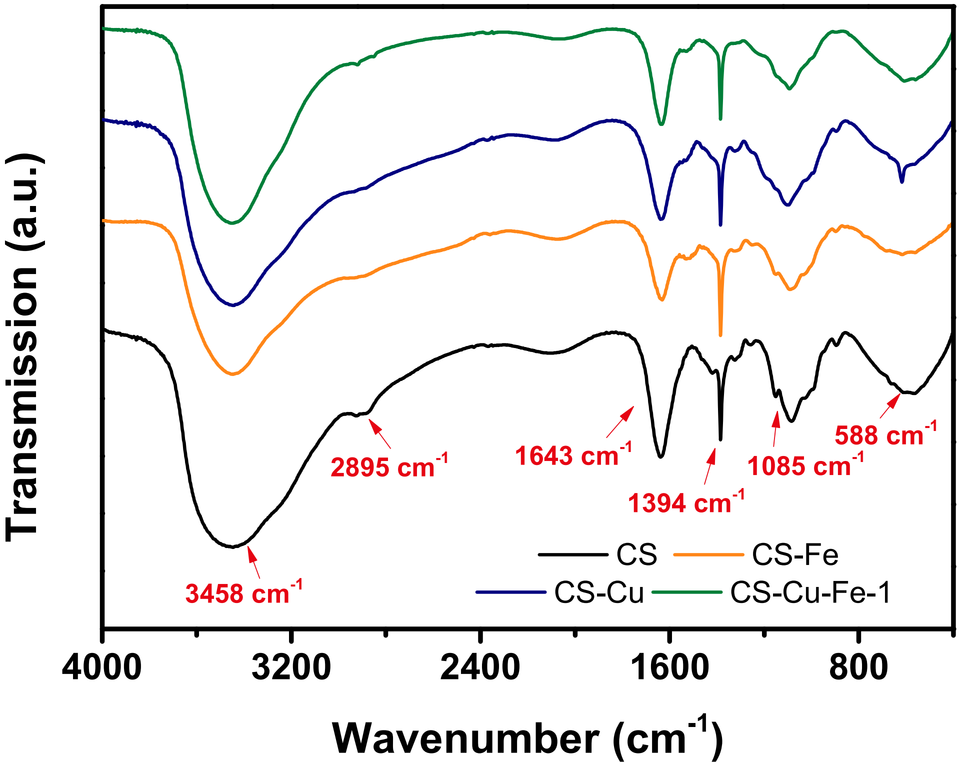
Transmission (a.u.)
Wavenumber (cm-1)
4000
3200
2400
1600
800
3458 cm-1
2895 cm-1
1643 cm-1
1394 cm-1
1085 cm-1
588 cm-1
CS
CS-Fe
CS-Cu
CS-Cu-Fe-1

Figure 8

1

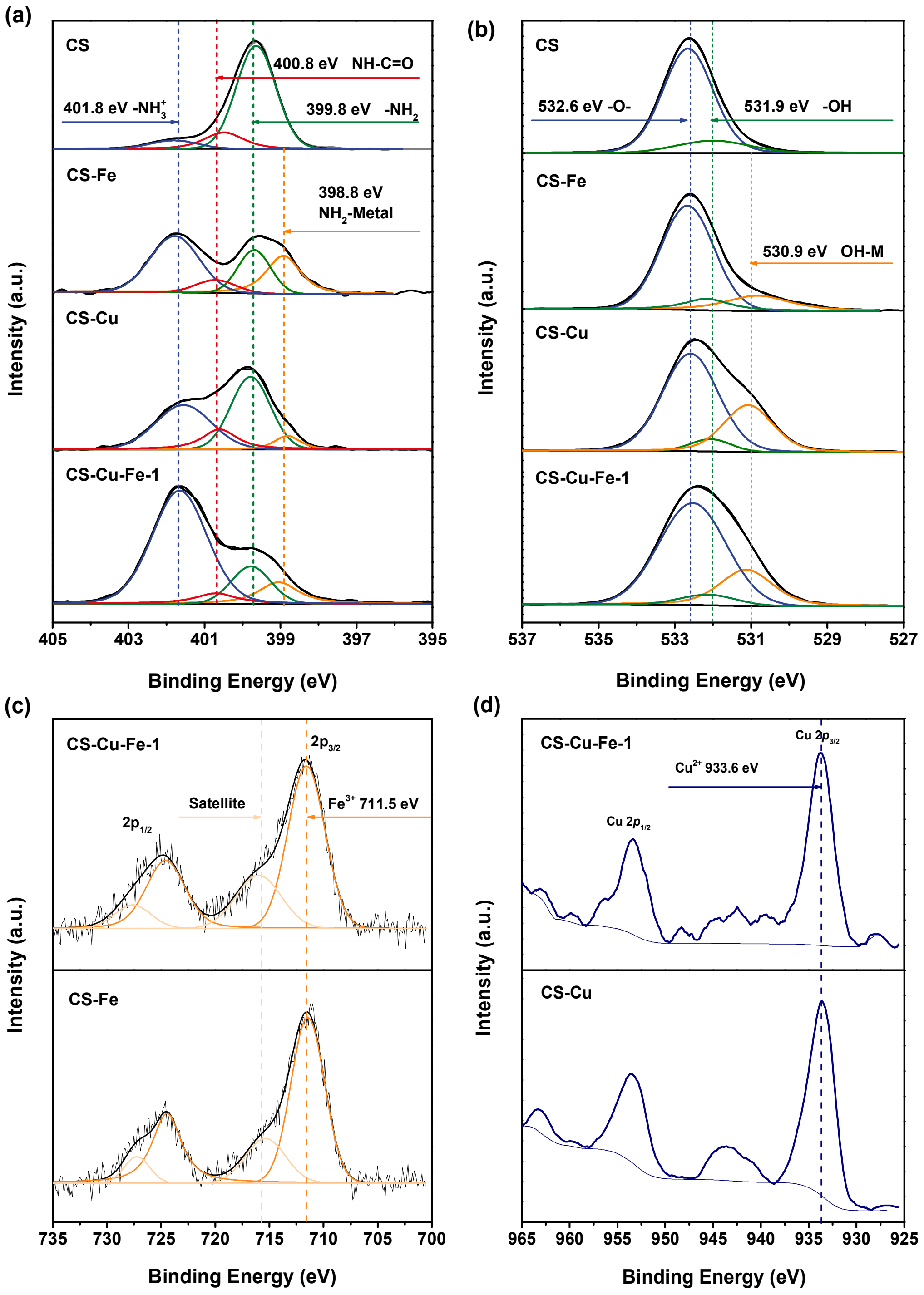
(a)
CS
400.8 eV NH-C=O
401.8 eV -NH$_3^+$
399.8 eV -NH$_2$
CS-Fe
398.8 eV
NH$_2$-Metal
CS-Cu
CS-Cu-Fe-1
Intensity (a.u.)
405
403
401
399
397
395
Binding Energy (eV)
(b)
CS
532.6 eV -O-
531.9 eV -OH
CS-Fe
530.9 eV OH-M
CS-Cu
CS-Cu-Fe-1
Intensity (a.u.)
537
535
533
531
529
527
Binding Energy (eV)
(c)
CS-Cu-Fe-1
2p$_{3/2}$
Satellite
Fe^{3+} 711.5 eV
2p$_{1/2}$
CS-Fe
Intensity (a.u.)
735
730
725
720
715
710
705
700
Binding Energy (eV)
(d)
CS-Cu-Fe-1
Cu 2$p_{3/2}$
Cu^{2+} 933.6 eV
Cu 2$p_{1/2}$
CS-Cu
Intensity (a.u.)
965
960
955
950
945
940
935
930
925
Binding Energy (eV)

Figure 9

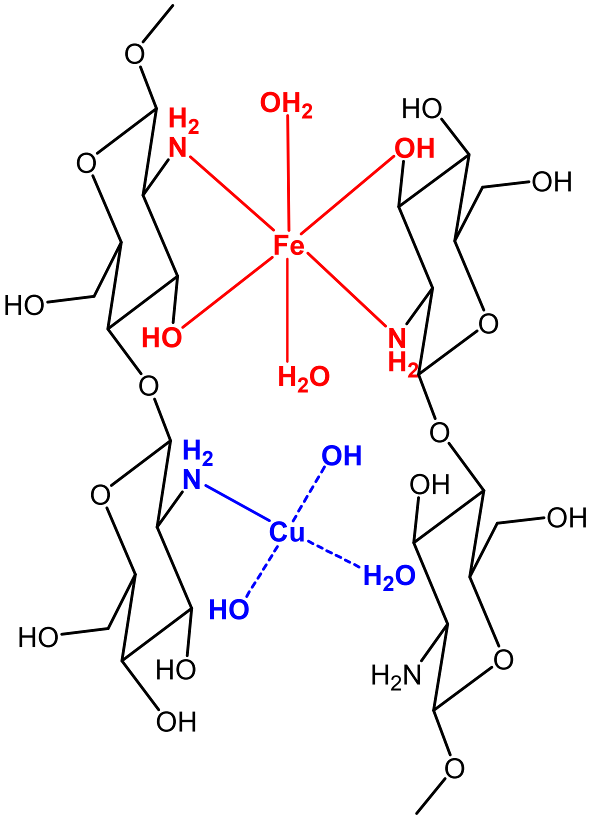
O
O
H2
N
OH2
HO
OH
OH
Fe
HO
HO
N
H2
O
H2O
O
O
H2
N
OH
OH
OH
O
Cu
H2O
HO
HO
HO
O
H2N
OH
O

Figure 10

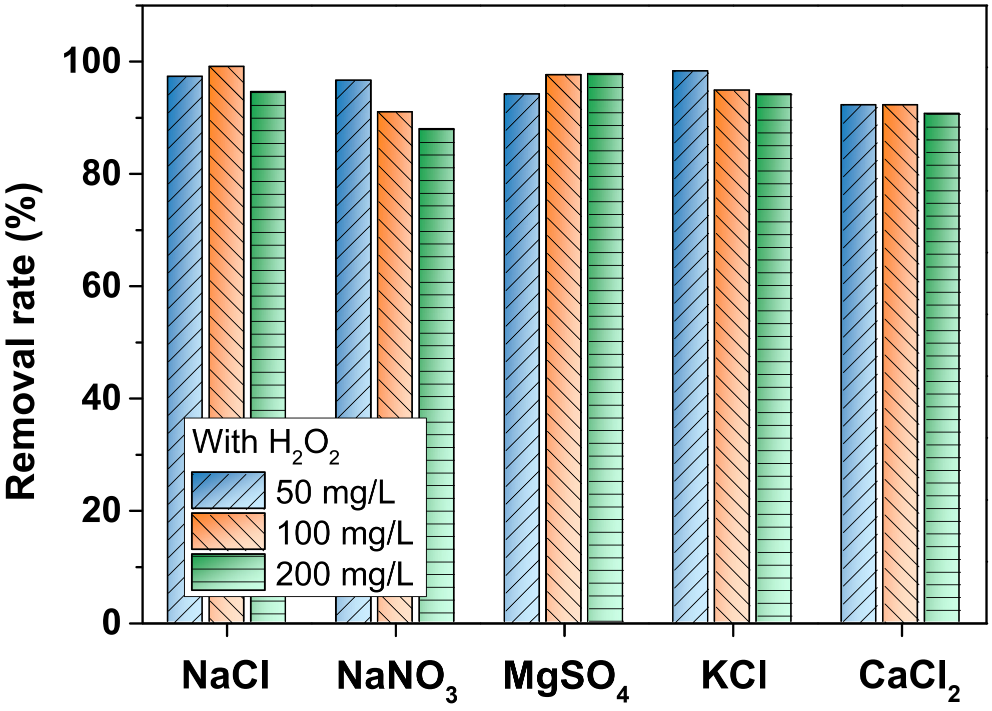
Removal rate (%)
0
20
40
60
80
100
With H_2O_2
50 mg/L
100 mg/L
200 mg/L
NaCl
$NaNO_3$
$MgSO_4$
KCl
$CaCl_2$

Figure 11

1

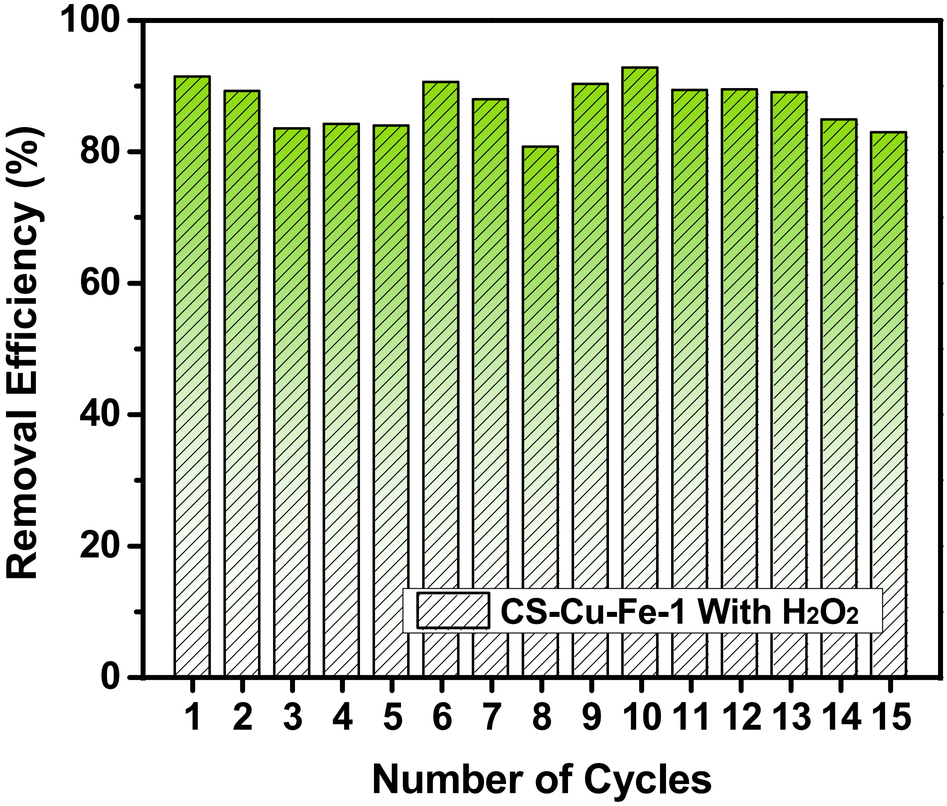
100
80
60
40
20
0
Removal Efficiency (%)
CS-Cu-Fe-1 With H2O2
1
2
3
4
5
6
7
8
9
10
11
12
13
14
15
Number of Cycles

Figure 12

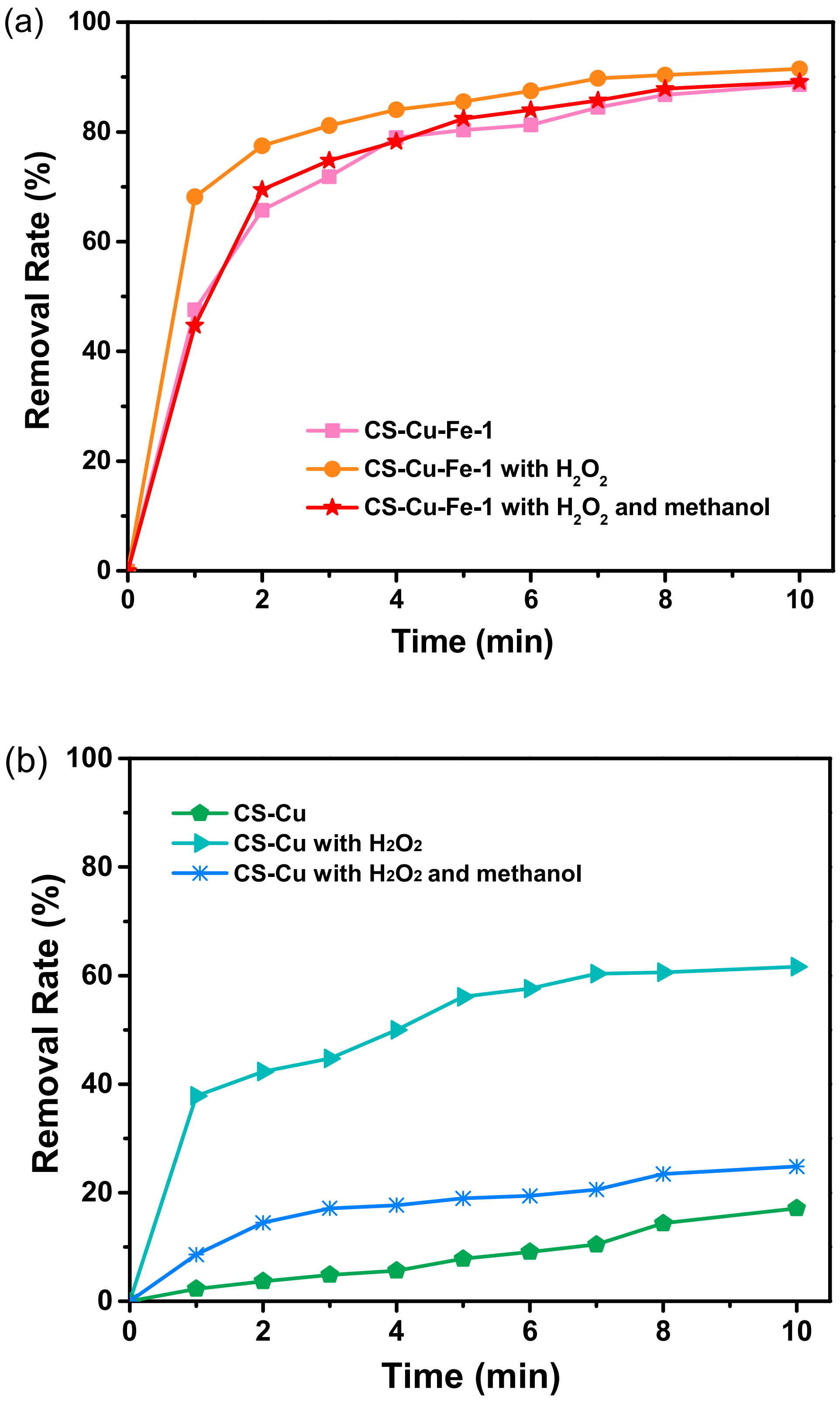
(a)
Removal Rate (%)
Time (min)
0
20
40
60
80
100
0
2
4
6
8
10
CS-Cu-Fe-1
CS-Cu-Fe-1 with H2O2
CS-Cu-Fe-1 with H2O2 and methanol
(b)
Removal Rate (%)
Time (min)
0
20
40
60
80
100
0
2
4
6
8
10
CS-Cu
CS-Cu with H2O2
CS-Cu with H2O2 and methanol

Figure 13